united nations
educational, scientific
and cultural
organization

international atomic
energy agency

the
abdus salam
international centre for theoretical physics

SMR/1270-23

SCHOOL ON SYNCHROTRON RADIATION

6 November – 8 December 2000

Miramare - Trieste, Italy

Supported in part by the Italian Ministry of Foreign Affairs in connection with the SESEME project

Co-sponsors: Sincrotrone Trieste, Società Italiana di Luce di Sincrotrone (SILS) and the Arab Fund for Economic and Social Development

Detectors

R. Menk
Sincrotrone Trieste
Italy

Image Formation and Detector Characterization

In x-ray radiographs image formation is a statistical process and the intrinsic limitations are given by Poisson noise only. A common measure of the image quality is the signal (S) to noise (σ) ratio (SNR_{out}) in the entire image or parts of the image.
Consider a homogeneous area A illuminated for a certain time T (a flat field image). At each single point of A a flux density, in the following denoted with $\phi(x,y,t)$, can be assumed to be superimposed with noise due to the poisson statistics. The signal to noise ratio within this illuminated area is then given by

$$SNR_{in} = \frac{\oint_A \int_0^T \phi(x,y,t) \cdot dt \cdot da}{\sqrt{\oint_A \int_0^T \phi(x,y,t) \cdot dt \cdot da}} = \frac{N}{\sqrt{N}} = \sqrt{N} \; . \qquad (1.)$$

N denotes the integral number of quanta in the entire area A. Note that this expression describes the intrinsic limitation for all kinds of photon imaging systems. An image of this area is recorded with an integrating detector. Photon integrating or, more precisely, energy integrating devices such as the discussed detectors contribute additional noise to the image. Thus, in general, the image information is degraded at each step of the detection. An image of the flat field recorded with a real, and hence noisy detector, delivers the following degraded SNR_{out}:

$$SNR_{out} = \sqrt{DQE} \cdot SNR_{in} \; . \qquad (2.)$$

Obviously, a reduced DQE value requires an increased number of quanta (or dose) in order to achieve the same signal to noise ratio in the recorded images. To avoid unnecessary dose applied to patients in this particular application, the DQE values of detector systems should be close to 1. With the knowledge of both the SNR_{out} and the SNR_{in} it is possible to evaluate the DQE for a given detector system. Images are sampled at discrete positions in the space domain with the period defined by the pitch of the segmentation. Obviously this kind of image recording underlies the sampling theorem and the smallest detail transmitted is defined by the 'Niquest frequency' in the reciprocal domain of the space. In the following this domain is denoted as the domain of spatial frequencies. Formula (2) can be rewritten in terms of the spatial frequencies f and g as

$$DQE(f,g) = \left(\frac{SNR_{out}(f,g)}{SNR_{in}(f,g)} \right)^2 = \left(\frac{S_{out}(f,g) \cdot \sigma_{in}(f,g)}{\sigma_{out}(f,g) \cdot S_{in}(f,g)} \right)^2 \qquad (3.)$$

where $SNR_{out}(f,g)$ and $SNR_{in}(f,g)$ are, respectively, the output and input signal to noise ratios at the spatial frequencies f and g. The transformation in the domain of the spatial frequencies allows the convenient evaluation of the DQE(f,g) in terms of experimental measurements. It will turn out that the input signal S_{in} as well as σ_{in} is independent of

spatial frequencies since the latter is considered to be white noise. Thus the SNR_{in} in the domain of the spatial frequencies is constant for all spatial frequencies. This can be shown by utilizing a pin hole aperture at the position x=0, y=0 which covers the flat field introduced earlier. The input signal in the spatial domain is then a convolution of the flux density with the pin hole which can be written in terms of a two dimensional Dirac distribution $\phi(x,y) \bullet \delta(x,y)$. One gets

$$S_{in}(x,y) = \int_{-\infty}^{\infty}\int_{-\infty}^{\infty} \phi(x,y)\cdot\delta(x,y)\cdot dx\cdot dy = \phi(0,0) = \phi_0 = \text{const} \qquad (4.)$$

and in the domain of the spatial frequencies

$$S_{in}(f,g) = c\cdot \int_{-\infty}^{\infty}\int_{-\infty}^{\infty} (\phi_0)\cdot e^{-i\cdot f\cdot x}\cdot e^{-igy}\cdot dx\cdot dy = \phi_0 \ . \qquad (5.)$$

c denotes the normalization of the transform and f and g are two base vectors of the spatial frequency domain. In the domain of the spatial frequencies the input noise in the Poisson case is

$$\sigma_{in}(f,g) = c\cdot \int_{-\infty}^{\infty}\int_{-\infty}^{\infty} \sqrt{\phi_0}\cdot e^{-i\cdot f\cdot x}\cdot e^{-igy}\cdot dx\cdot dy = \sqrt{\phi_o} \qquad (6.)$$

which results in $SNR_{in}(f,g) = \sqrt{\phi_0}$.

The detector system, however, responds to the input impulse at the object coordinates x = y = 0 with a characteristic transfer function. Due to the effects of charge generation within the detector the ionization which consists of the image information does not necessarily remain at this specific position but rather spreads over adjacent pixels. This causes a blurring or enlargement of the signal at the image coordinates x', y'. This effect is described by the point-spread-function (PSF). Mathematically the output signal S_{out} in the space domain of the image is a convolution of the input signal with the PSF of the detector and with the quantum efficiency ε of the detector. One gets

$$S_{out}(x',y') = \varepsilon\cdot \int_{-\infty}^{\infty}\int_{-\infty}^{\infty} \phi(x,y)\cdot\delta(x,y)\cdot PSF(x-x',y-y')\cdot dx\cdot dy = \qquad (7.)$$

$$\varepsilon\cdot\phi(0,0)\cdot PSF(-x',-y') = \varepsilon\cdot\phi_0\cdot PSF(x',y')$$

The latter equality is allowed since the PSF is symmetric by definition. A Fourier transform delivers the output signal in terms of its spatial frequencies and one obtains

$$S_{out}(f,g) = c\cdot\varepsilon\cdot \int_{-\infty}^{\infty}\int_{-\infty}^{\infty} \phi_0\cdot PSF(x',y')\cdot e^{-i\cdot f\cdot x'}\cdot e^{-igy'}\cdot dx'dy' = c\cdot\phi_0\cdot MTF(f,g) \qquad (8.)$$

where MTF is the modulation transfer function. In practice the MTF is a measure of how well a detail of a certain size is recorded with the detector system. Note that for an ideal detector MTF(f,g) = 1 at all spatial frequencies. For such a detector the noise would be independent of spatial frequencies, similar to the input noise in formula (6). The low pass characteristics of a real detector, however, degrade the high spatial frequency signals as

well as the high frequency noise. In general the image noise recorded with an integrating detector can be subdivided into two major constituents: one part due to the Poisson statistics, and a second additional noise source in the following denoted with σ_{add} . The latter consists of inherent detector noise, electronics noise and ADC noise, which add in quadrature since they are statistically independent. In the model developed so far the total image noise in the space domain would be

$$\sigma_{tot}^2 = \varepsilon \cdot \phi_0 + \sigma_{add}^2 \tag{9.}$$

when ε is the quantum efficiency of the detector. In this notation σ_{add} has the dimension of a photon flux at the input of the detector. The Fourier transform of (8) delivers directly the noise power spectrum NPS(f,g)

$$\begin{aligned} NPS(f,g) &= \left|\Im(\sigma_{tot}^2)\right| = c_1 \cdot \int_{-\infty}^{\infty}\int_{-\infty}^{\infty} (\phi_0 \cdot \varepsilon)\, e^{-i\cdot f\cdot x} \cdot e^{-igy} \cdot dx \cdot dy + c_2 \cdot \int_{-\infty}^{\infty}\int_{-\infty}^{\infty} \sigma_{add}^2 \cdot e^{-i\cdot f\cdot x} \cdot e^{-igy} \cdot dx \cdot dy \\ &= W_p + W_d \end{aligned} \tag{10.}$$

W_p and W_d are the so called Wiener spectrum of the Poisson noise and the additional noise, respectively and c1 and c2 some normalization constants. From equations (5), (6) , (8) and (10) an expression for the DQE is

$$DQE(f,g) = \varepsilon \cdot c^2 \cdot \phi_0 \cdot \frac{|MTF(f,g)|^2}{NPS(f,g)} = \chi(\phi_0) \cdot \frac{|MTF(f,g)|^2}{NPS(f,g)} \tag{11.}$$

or for the one dimensional case

$$DQE(f) = \varepsilon \cdot c^2 \cdot \phi_0 \cdot \frac{|MTF(f)|^2}{NPS(f)} = \chi(\phi_0) \cdot \frac{|MTF(f)|^2}{NPS(f)} \quad . \tag{11.a}$$

$\chi(\phi_0)$ is a detector property which relates variations in detector exposure at zero spatial frequency to variations at the output and is often interpreted as Zero Spatial Frequency DQE (ZSFDQE) which can be defined as

$$\chi(\phi_0) = \left(\frac{SNR_{out}(\phi_0)}{SNR_{in}(\phi_0)}\right)^2 . \tag{12}$$

In the following an expression for the zero spatial frequency DQE is developed with special regard to photon or, more appropriate, to energy integrating detectors. In the discussion it is more convenient to deal with photon numbers than flux densities. With a pixel width of b, a beam or pixel height of a and an integration time T for a flux density ϕ, an integrated number of N photons are measured in a particular pixel with an associated error of $\sqrt{N}$ leading to $SNR_{in} = \sqrt{N}$. As mentioned above the detectors are

energy integration rather than photon integration devices. Taking this into account, the total charge released in a particular detector pixel by N photons of the energy E_γ is

$$Q = \frac{E_{ab}}{W_{ion}} \cdot N \cdot e. \tag{13}$$

Here $E_{ab} = FE_\gamma$ denotes the total absorbed energy in a detector element, and W_{ion} is the ionization energy required to produce an ion - electron pair (or one electron - hole pair). F is the Fano factor that takes into account that not all the energy carried by a photon is really deposited in the detector and hence F is always less than one. The output signal is $S_{out}=kQ\varepsilon$, where k is a property of the acquisition electronics that describes the conversion of charge to gray values in the image. An error propagation eventually leads to the total image noise σ_{out}

$$\sigma_{out} = \sqrt{Q^2 \cdot \left(\varepsilon^2 \cdot k^2 \cdot \frac{\int_0^\infty n(E) \cdot E^2 \cdot dE}{N \cdot E^2} + \varepsilon \cdot k^2 \cdot \frac{1}{N} \right) + \sigma_{add}^2} \tag{14}$$

The first term in brackets describes normalized fluctuations of the absorbed energy spectrum n(E) in the pixel with

$$E_\gamma = \int_0^\infty n(E) \cdot E \cdot dE.$$

The second term is the error due to the Poisson fluctuations. Other possible noise sources lsuch as electronics noise, ADC noise and the inherent detector noise have been taken into account by the additional noise term σ_{add}. Formula (12) and (14) eventually lead to the following expression of the ZSFDQE

$$\chi(\phi) = \frac{\varepsilon}{1 + \frac{\varepsilon \cdot \int_{-\infty}^{\infty} n(E) \cdot E^2 \cdot dE}{E^2} + \frac{\sigma_{add}^2 \cdot W_{ion}^2}{\varepsilon \cdot k^2 \cdot F^2 \cdot E_\gamma^2 \cdot \phi \cdot e^2 \cdot T \cdot a \cdot b}}. \tag{15}$$

Formula (15) reveals four characteristics of the ZSFDQE:

1. For high photon fluences the expression is dominated by the quantum efficiency ε of the detector. Obviously ZSFDQE values close to 1 are achievable by detectors with a high absorption efficiency only.
2. Most of the absorbed energy should really remain in the pixel in which the ionization took place. Ideally, the integral in the denominator should vanish if the overall ionization can be localized in a single pixel. Fluorescence photons that escape from a considered

pixel will cause a spread in the energy spectrum which results in an increase of the fluctuations and a decrease of the ZSFDQE .
3. Since the additional noise term shifts the ZSFDQE rather than changing its shape, σ_{add} should be as low as possible in order to achieve high ZSFDQE values even for small photon fluences.
4. In principle the same effect on the ZSFDQE as described in 3. is valid for the ionization energy W_{ion} with the exception that low ionization energies carry the disadvantage of thermal charge production. This statistical process contributes to the additional noise term.

Further reading

J.C.Dainty and R.Shaw, Image Science, Academic, New York, 153, (1974)

D. Chapman, C.Schultz, IEEE Conference Report, Nuclear Science Symposium and Medical Imaging Conference, Vol III, (1993), 1528

K.Doi et al, "MTF's and Wiener Spectra of Radiographic Screen-Film Systems", U.S.Dept. of Health and Human Service Publ. FDA 82 - 8187, (1992)

R.M.Nishikawa and M.J.Yaffe," Signal to Noise Properties of Mammographic Film Screen Systems", Med.Phys. 12 (1), 32 (Jan./Feb. 1985)

Radiation detection and measurements, Glen Knoll, John Wiley and Sons, New York

Detectors for Synchrotron Radiation 1

Ralf -Hendrik Menk
Sincrotrone Trieste
Instrumentation

Introduction: Life with Detectors

Theory

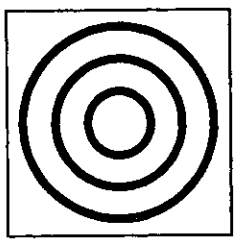

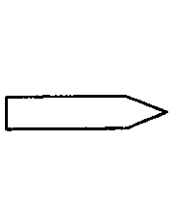

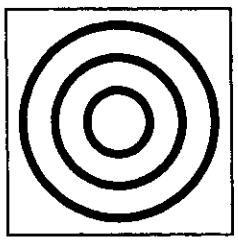

Expected signal (lipid diffraction ring)

Recorded signal

Daily Life

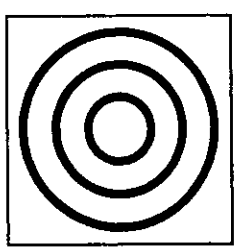

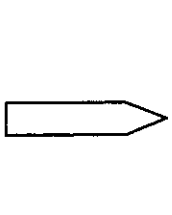

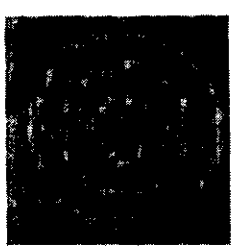

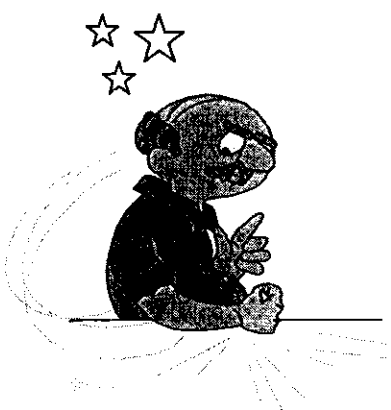

Expected signal

Recorded signal

Outline

- First lecture
  - and some theory
  - and detector quantum efficiency
- Second lecture
  - some application
  - integrating and spectroscopic systems

Introduction: some troubles of real detectors

Trouble	Correcting methods
Noise	No chance
Saturation effects	No chance
Pick ups	Hardly correctable
Dead-time losses	Partially correctable
Multi element detectors	
Image distortions	Sometimes correctable
Single channel response	Correctable if linear
Dark currents	Partially correctable

Quantum efficiency ε

$$\varepsilon := \frac{\text{no of photons that interact in the detector volume}}{\text{no of photons in front of the detector}}$$

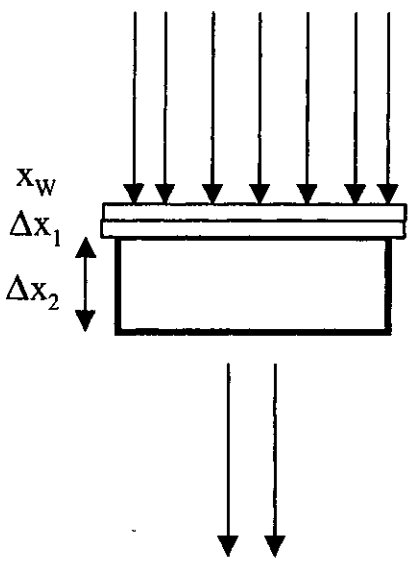

I_0

Detector window and/or
'dead volume'

Conversion volume
defined by ρ and μ

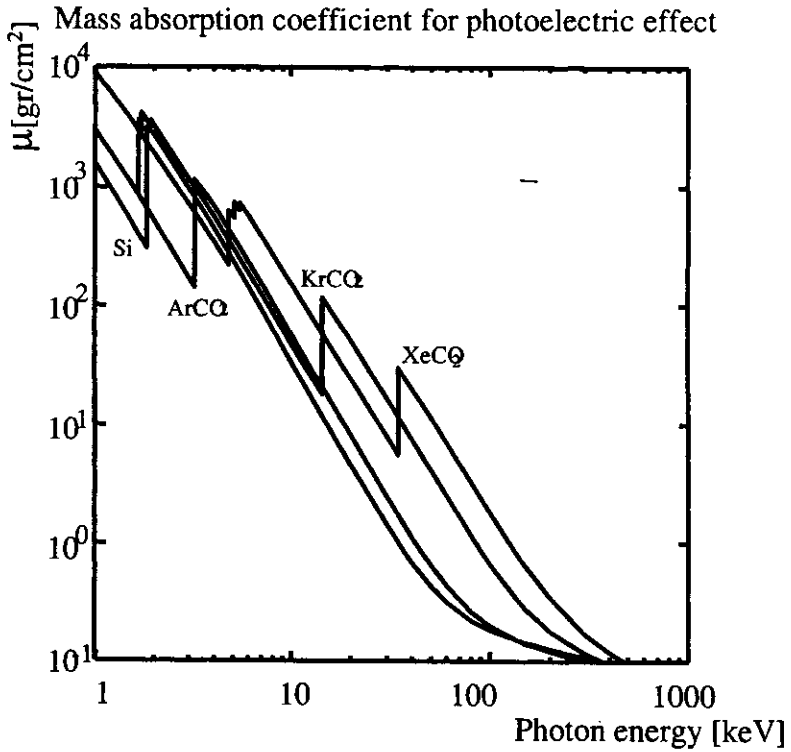

More suitable: energy efficiency ε_E

Example: gaseous detector-. Ionization chamber

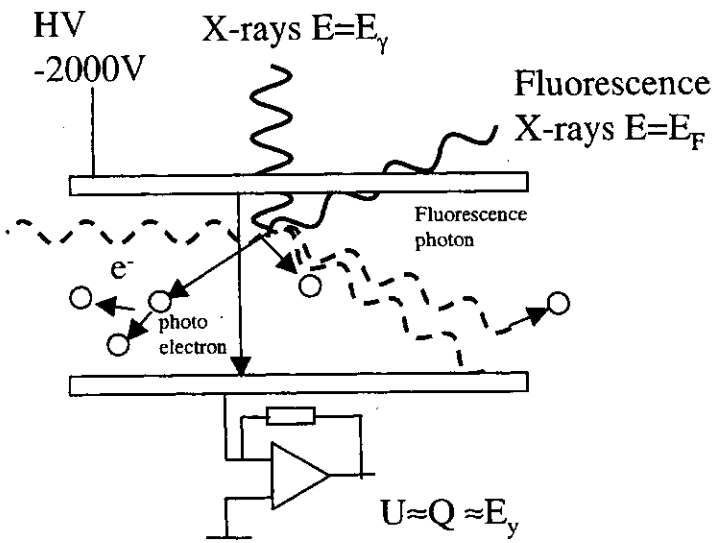

Process	Energy
photo electron	$E_p = E_y - E_b$
Fluorescence photon	$E_f = E_i - E_i$
Auger electron	$E_a = E_k - 2E_l$ for photo effect on k-shell

Gas	W_{ion}[eV] energy to generate Ion /e
Ar	26
Kr	24
Xe	22

Example: E_y = 8000 eV , conversion gas Xe

n^- := no of electrons per converted photon

$n^- = E_y / W_{ion} \Rightarrow Q = e^- E_y / W_{ion}$

$n^- = 364$ electrons , $Q = 5.81 * 10^{-17}$ C

Typical 'energy spectrum'

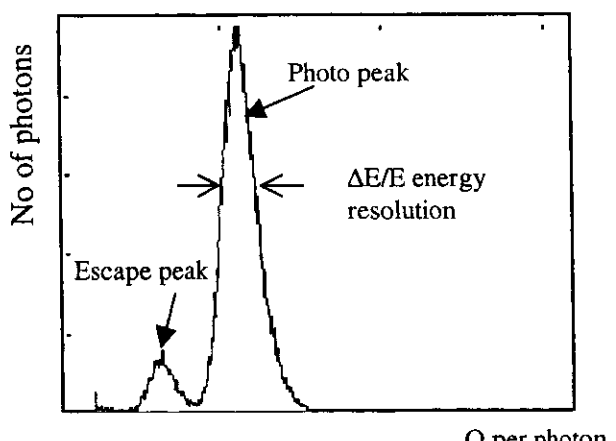

Spatial resolution

'Dirac' needle

Detector response PSF/LSF

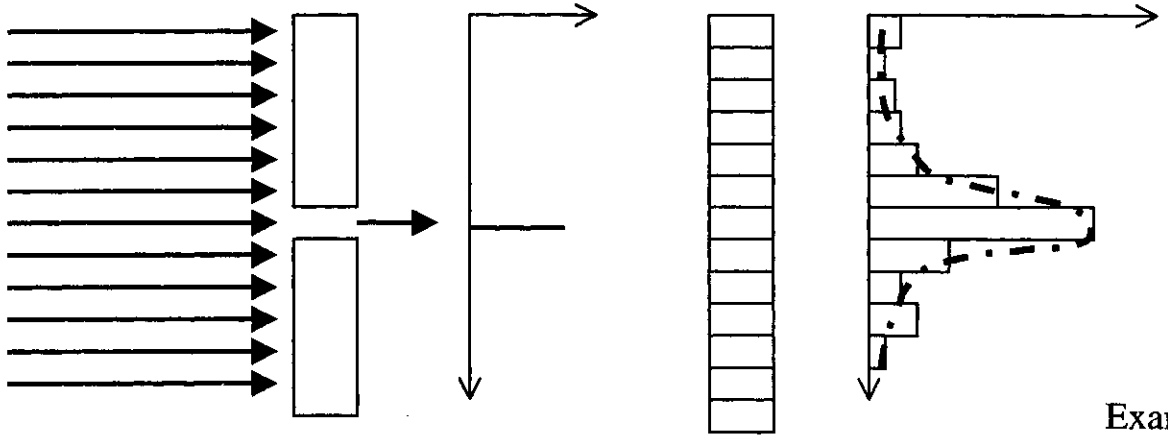

Signal smearing is due to
- the process of charge generation
- and the discrete pixel size

Example: gaseous detector-. Ionization chamber

Slit system

Segmented detector

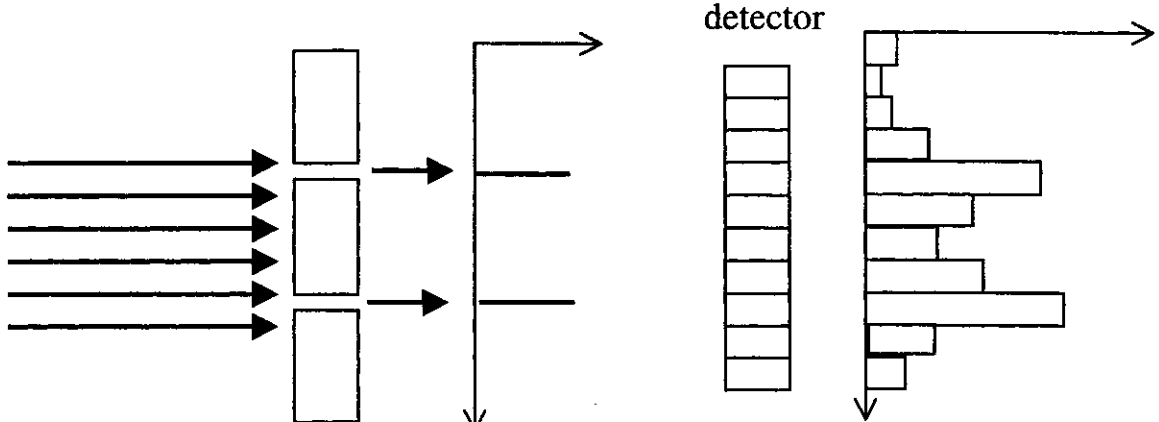

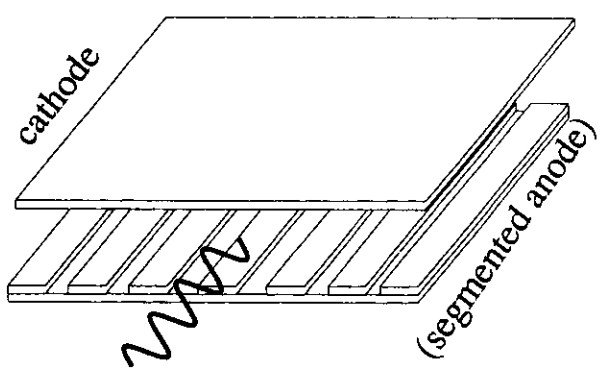

Spatial resolution: charge generation and Point Spread Function

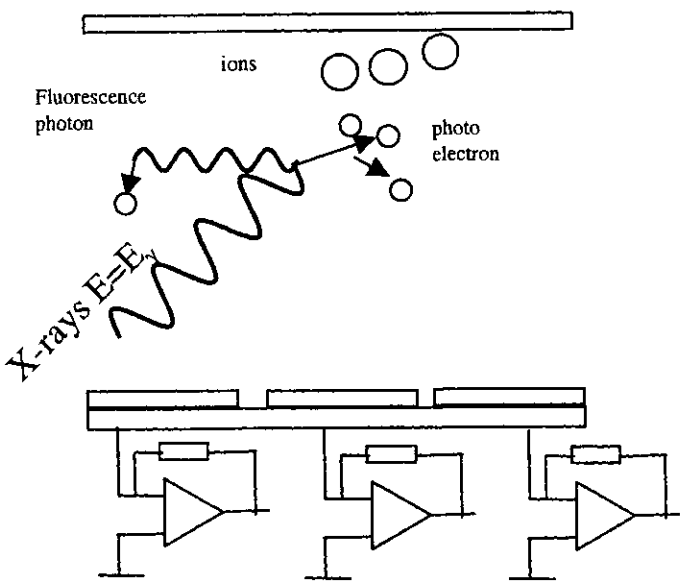

Contributions o the spatial resolution

- Range of photo electrons
- diffusion of the electron components
- range of the fluorescence
- pixel size of the segmentation
- electronics cross talk
- induction of ion component
- etc

$$PSF(x) = \int_{-\infty}^{\infty} [.[\int_{-\infty}^{\infty} \delta(x'..') \cdot g_1(x'..')dx'..'].] \cdot g_n(x - x')dx'$$

$$= \delta * g_1 * .... * g_n$$ Point Spread Function /Line Spread Function

Spatial resolution: range of photo electrons in gases

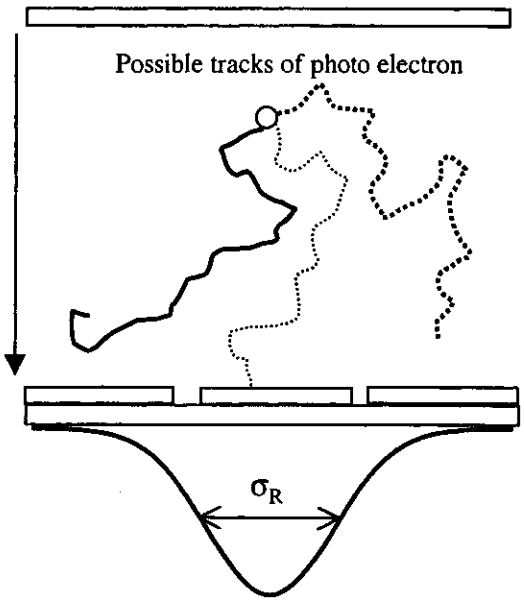

Projected distribution of photo electrons on the segmented electrode

$$r_p(x) = e^{-\frac{x^2 \cdot \rho_{gas}^2}{2 \cdot \sigma_R^2}}$$

$$\sigma_R = 1.5 \cdot 10^{-3} \cdot E_{kin}^{1.75}, \dim(\sigma_R) = \left[\frac{mgr}{cm^2}\right], \dim(E_{kin}) = [keV]$$

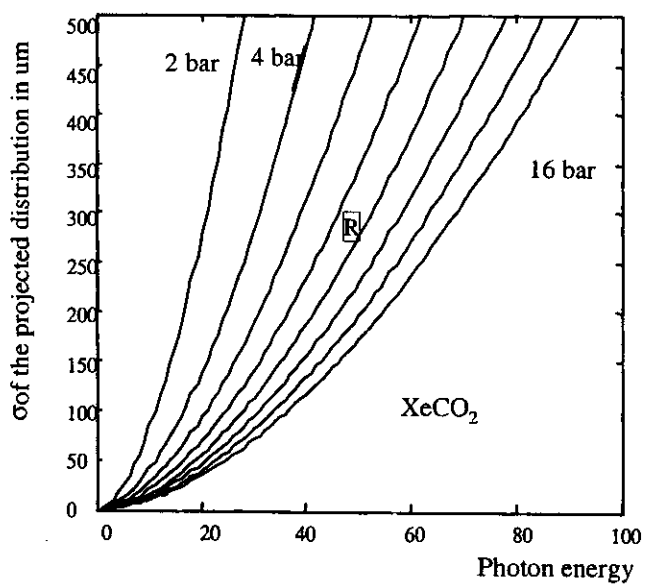

Spatial resolution: diffusion of the electrons

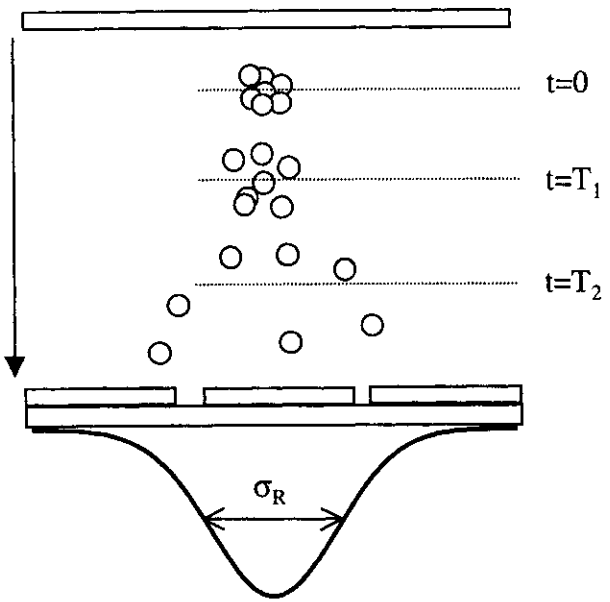

$$d(x) = e^{-\frac{x^2}{4\cdot\sigma_D^2}}$$

$$\sigma_D = \sqrt{2\cdot D_t \cdot t} = \sqrt{\frac{2\cdot D_t \cdot z_{drift}\cdot P}{\mu^- \cdot E}}$$

- D_t Diffusion constant
- E electrical field
- P pressure
- u- mobility
- z_{drift} drift distance
- t drift time

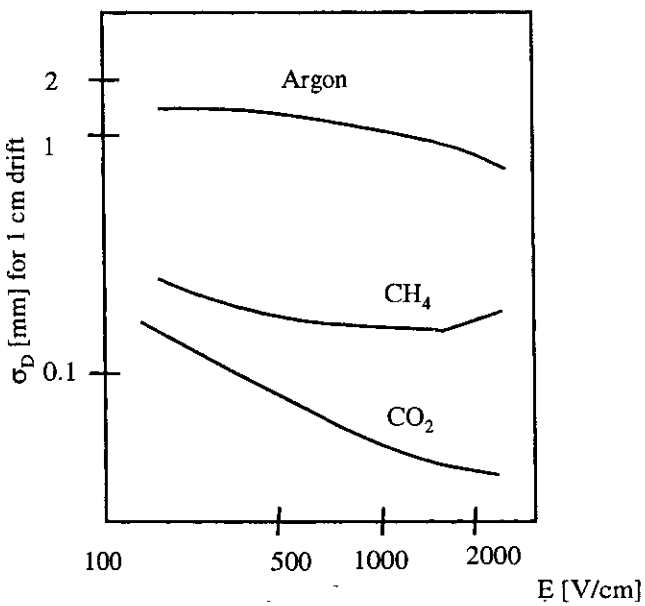

Spatial resolution: Fluorescence and pixel size

Fluorescence strongly depends on the geometry gas, energy etc. -> no analytical expression -> Monte Carlo

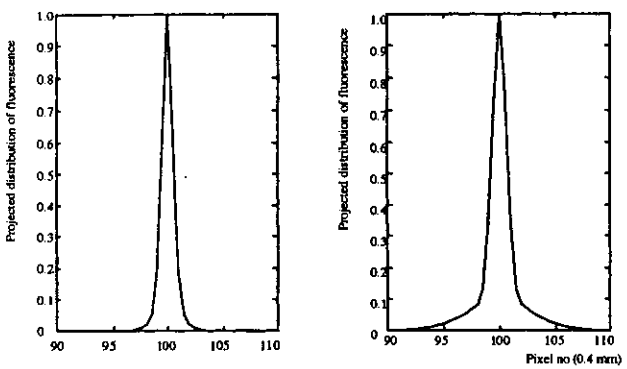

For Kr-CO_2 filled Ionization chamber
with a pixel size of 0.4mm and E_y= 33.174 keV
Distance anode -cathode = 3 mm / 10 mm

Pixel size

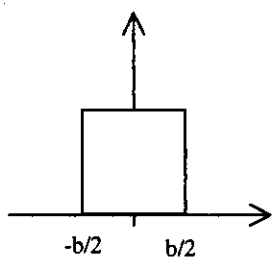

$$g(x)=\begin{cases}\frac{1}{b} & for\ -\frac{b}{2}<x<\frac{b}{2}\\ 0 & else\end{cases}$$

σ_p = b/sqrt(12)

Periodic repetition of pixels in real detector

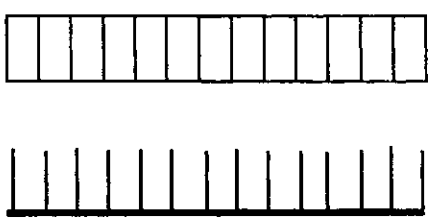

Dirac Comb

Segmentation is a convolution of g(x) with Dirac comb

Spatial resolution: Nyquist Sampling Theorem

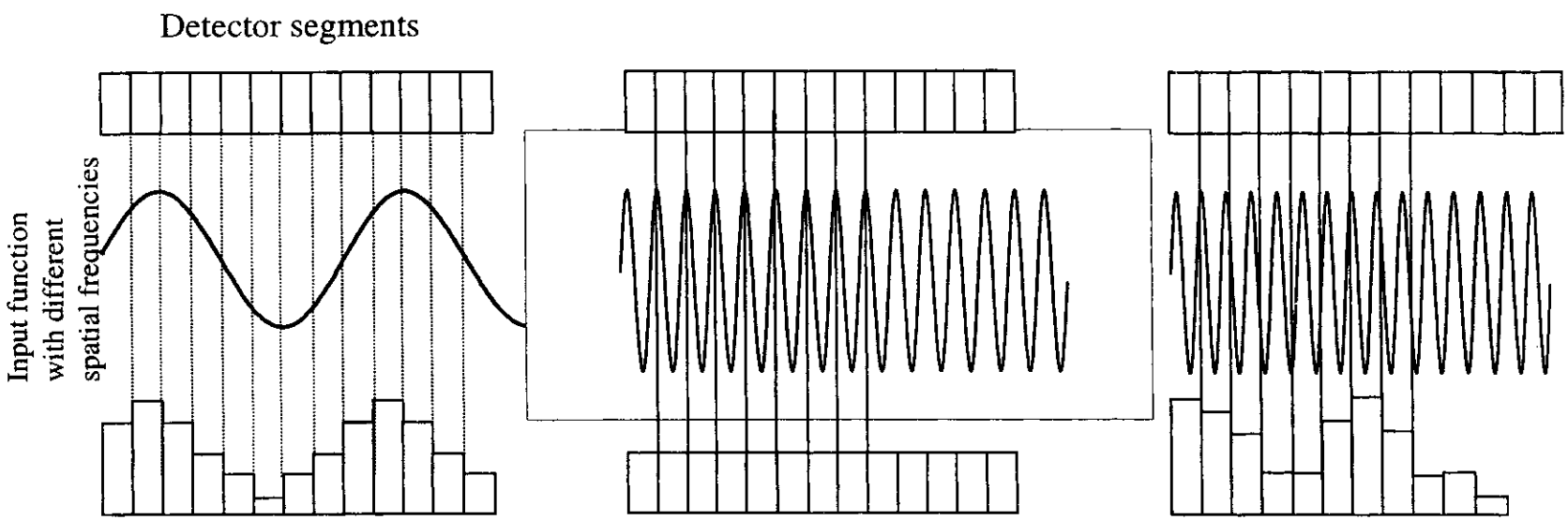

How good are different spatial frequencies transmitted (modulated) by the detector??

$$PSF(x)=\begin{cases}\frac{1}{b} & for -\frac{b}{2}<x<\frac{b}{2}\\ 0 & else\end{cases}$$

Transformation in Fourier space

$$MTF(u)=\left|\int_{-\infty}^{\infty} PSF(x)\cdot e^{-2\pi iux}\cdot dx\right| \longrightarrow \mathrm{MTF(u)}=\left|\frac{\sin(2\cdot\pi\cdot u\cdot b)}{2\cdot\pi\cdot u\cdot b}\right|$$

MTF = Modulation Transfer Function

Spatial resolution: Modulation Transfer Function

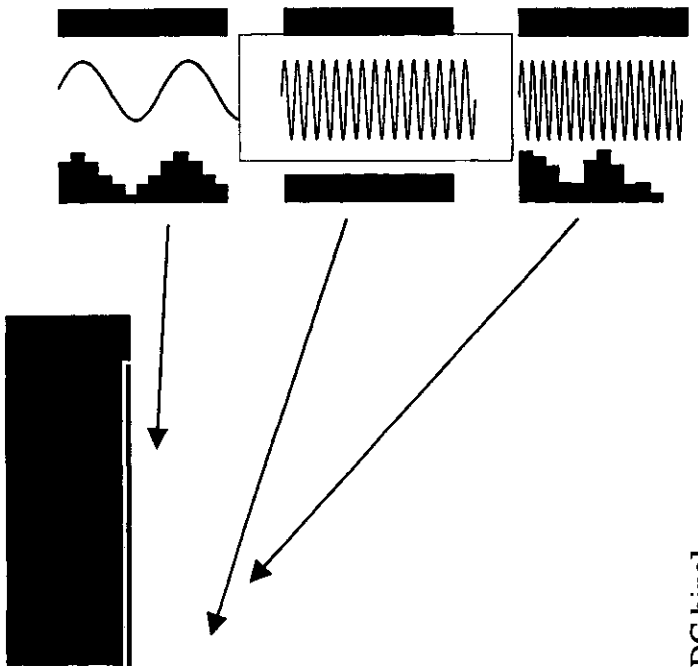

Spatial frequencies LP/mm

Open
open

10LP/mm

8LP/mm

4LP/mm

3LP/mm

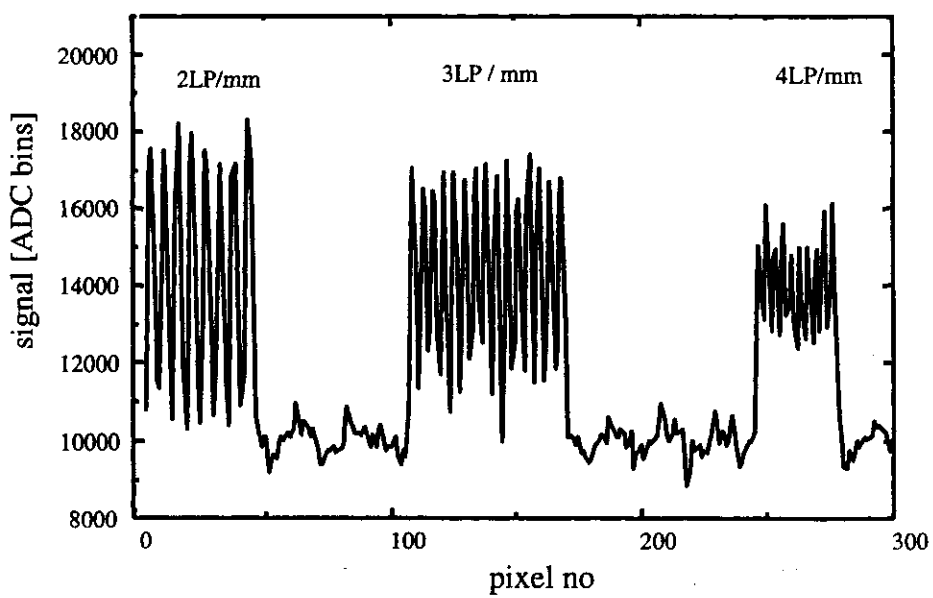

Detective Quantum Efficiency : Signal to Noise Ratio

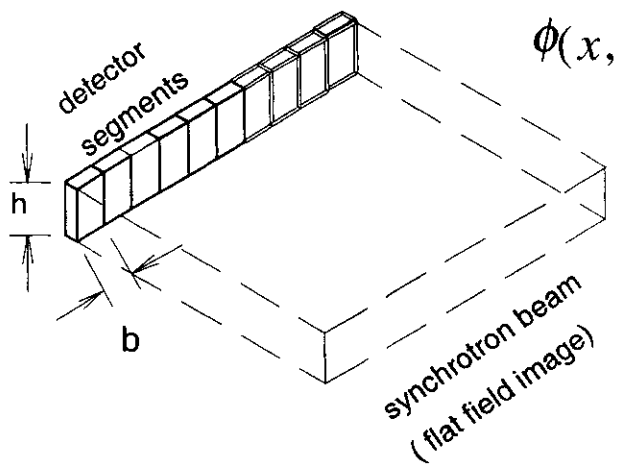

$$\phi(x, y, t) = \phi_0 = const$$

$$S_{in} = \iiint \phi(x, y, t) \cdot dx \cdot dy \cdot dt$$

$$= \phi_0 \cdot h \cdot b \cdot T = N$$

$$\sigma_{in} = \sqrt{N}$$

$$SNR_{in} = \frac{S_{in}}{\sigma_{in}} = \sqrt{N}$$

Detective Quantum Efficiency : Signal to Noise Ratio for integrating detectors

$$S_{out}(x) = \varepsilon \cdot S_{in}(x) \otimes PSF(x) = \varepsilon \cdot N(x) \otimes PSF(x)$$

$$\sigma_{out} = \sqrt{\varepsilon \cdot N \otimes PSF(x) + \sigma^2_{add}}$$

$$SNR_{out} \frac{\varepsilon \cdot N(x) \otimes PSF(x)}{\sqrt{\varepsilon \cdot N \otimes PSF(x) + \sigma^2_{add}}}$$

$$SNR_{out} = \sqrt{DQE} \cdot SNR_{in}$$

$$DQE = \left(\frac{SNR_{out}}{SNR_{in}} \right)^2$$

Detective Quantum Efficiency for integrating detectors

$$\Im(DQE) = \Im\left(\left(\frac{SNR_{out}}{SNR_{in}}\right)^2\right)$$

MTF = modulation transfer function
NPS = noise power spectrum
$\chi(N)$ = zero spatial frequency DQE

$$\Im(DQE) = DQE(f) = \frac{\Im\left(\varepsilon \cdot N \otimes PSF(x)\right)}{\Im\sqrt{\left(\varepsilon \cdot N \otimes PSF(x) + \sigma^2_{add}\right)^2} N} =$$

$$= \chi(N) \frac{|MTF(f)|^2}{NPS(f)}$$

$$DQE(f,N) = \frac{\varepsilon}{1 + \frac{\sigma^2_{add}}{\varepsilon \cdot N}} \frac{|MTF(f)|^2}{NPS(f)}$$

Detective Quantum Efficiency for counting detectors: dead time

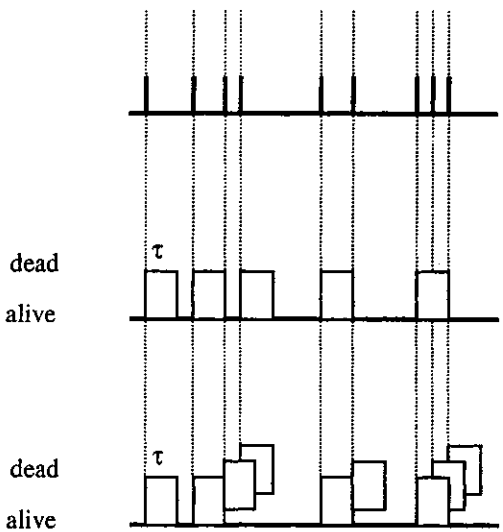

m = measure rate
n = real rate
τ = dead time
Events in the detector

Non paralyzable

$m = n/(1+n\,\tau)$

Paralyzable

$m = ne^{-n\tau}$

$$\chi(f=0) = \left(\frac{SNR_{out}}{SNR_{in}}\right)^2$$

$$S_{out} = \frac{n}{1+n\cdot\tau}, \quad \Delta S_{out} = \sqrt{\frac{n}{1+n\cdot\tau}}$$

$$SNR_{out}^2 = \frac{n}{1+n\cdot\tau}$$

$$S_{in} = n; \quad \Delta S_{in} = \sqrt{n}$$

$$SNR_{in}^2 = n$$

$$\boxed{\chi(f=0) = \frac{1}{1+n\cdot\tau}}$$

Detective Quantum Efficiency

Integrating detectors

$$DQE = \frac{\varepsilon}{1 + \frac{\sigma_{add}^2}{\varepsilon \cdot N}} \cdot |MTF|^2$$

— Integrating detector 10 photon noise equivalent per integration time

····· Integrating detector 100 photon noise equivalent per integration time

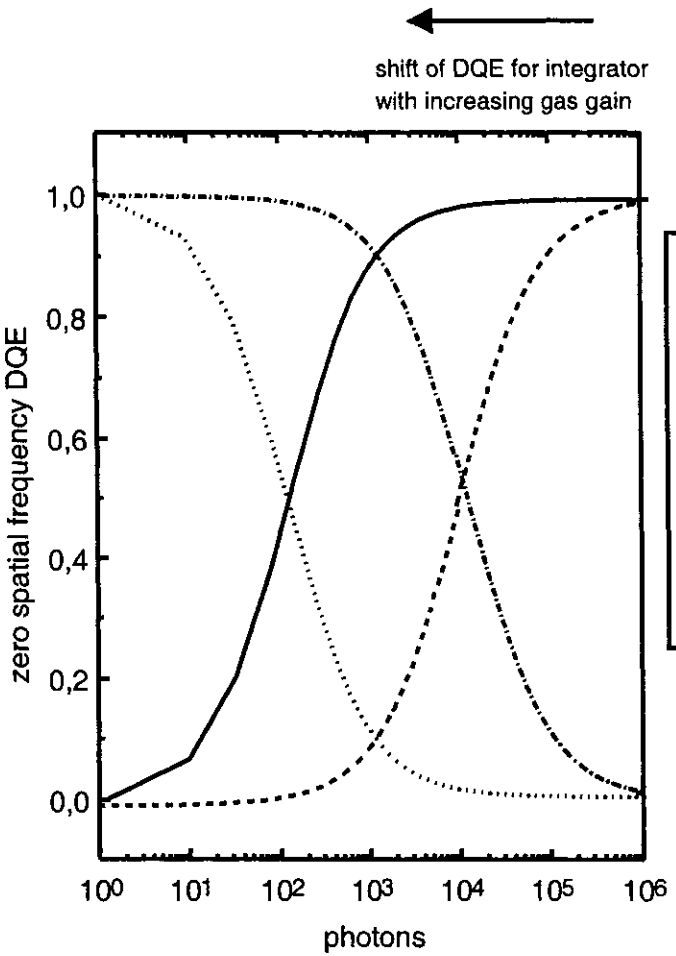

Counting detectors

$$DQE = \frac{\varepsilon}{1 + R \cdot \tau} \cdot |MTF|^2$$

– · – counter 1µs dead time

····· Counter 1ms dead time

Saturation recombination

$$f = \frac{1}{1 + \frac{1}{6} \cdot m^2 \cdot \Gamma^{-2}}, \quad m = \sqrt{\frac{\alpha}{\mu^+ \cdot \mu^- \cdot e}}, \quad \Gamma = \frac{V}{d^2 \cdot \sqrt{q_o}}$$

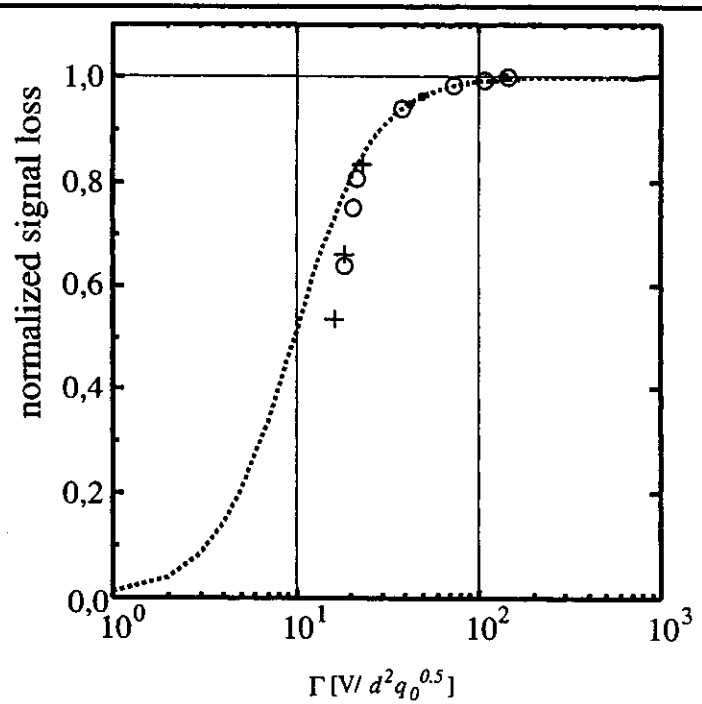

○ measurements

\+ Simulation with space charges

····· Boag model with m = 24 for Xe

Xe,d=3mm, E=33keV,p=10 bar > 10^{12} photons s^{-1} mm^{-1}

Boag J.W. *Ionization Measurements at very high Intensities*, 1950 Brit. Rad. Radiol., XXIII, Vol.274,p.601

Detectors for Synchrotron Radiation (2)

Ralf -Hendrik Menk
Sincrotrone Trieste
Instrumentation

Which devices are available?

Integrating detectors

- Ionization chambers
- Ionization chambers with gas gain
- .....

Gaseous Detectors

counting detectors

- Avalanche detectors
- streamer resistive plate chambers
- spark chambers
- ....

Spectroscopic detectors

- wire chambers (RAPID)
- micro pattern detectors
  - micro strip gas chambers
  - CAT, Micro CAT
  - Micro megas
  - GEM ....

Ionization chamber: Application: Transvenous Coronary Angiography

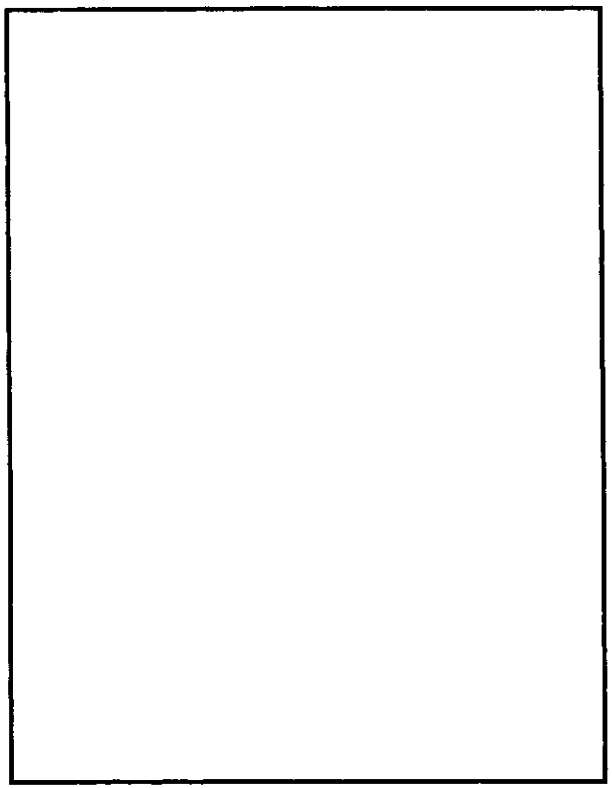

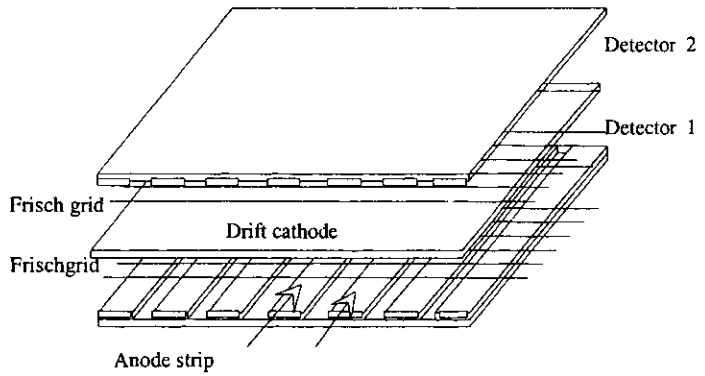

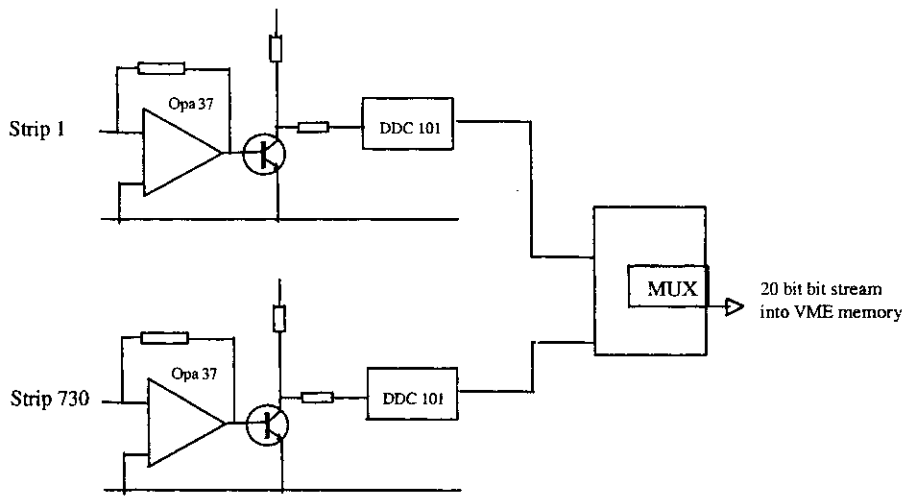

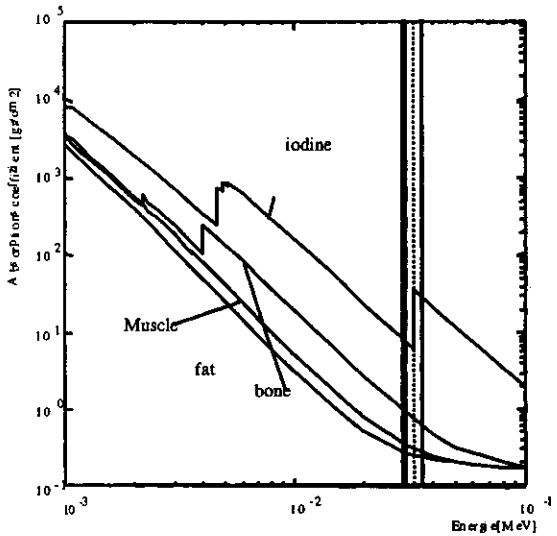

$$\begin{pmatrix} S_{water} \\ S_{iod} \end{pmatrix} = \begin{pmatrix} \rho_w \cdot \Delta x_w \\ \rho_i \cdot \Delta x_i \end{pmatrix} = \begin{pmatrix} \frac{1}{\mu_w^>} \cdot \left(1 - \frac{\mu_i^>}{\mu_i^> - \mu_i^<}\right) & \frac{\mu_i^>}{\mu_w^<} \\ \frac{1}{\mu_i^> - \mu_i^<} & \frac{1}{\mu_i^> - \mu_i^<} \end{pmatrix} \cdot \begin{pmatrix} -\ln\left(\frac{\phi_1}{\phi_{01}}\right) \\ -\ln\left(\frac{\phi_2}{\phi_{02}}\right) \end{pmatrix}$$

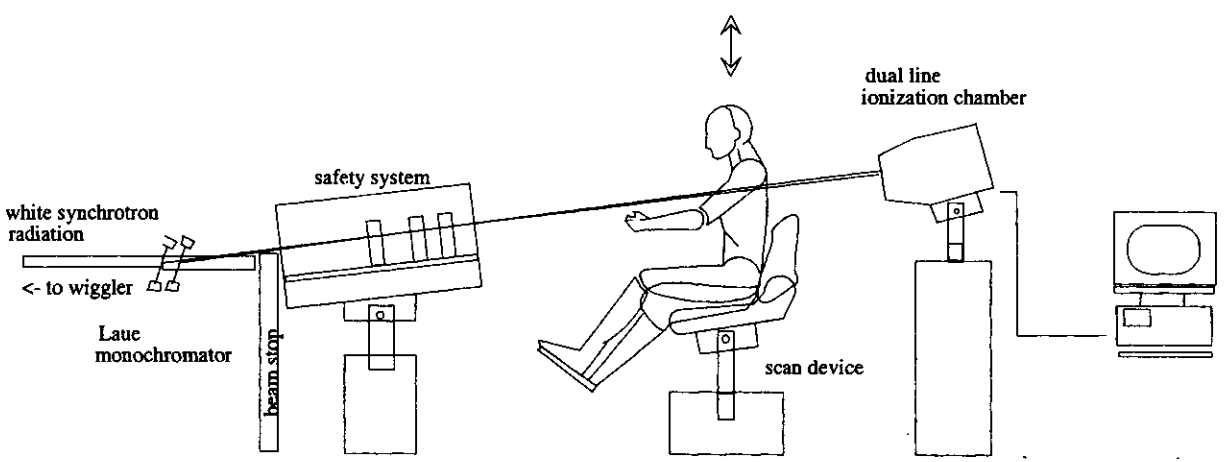

Low energy image

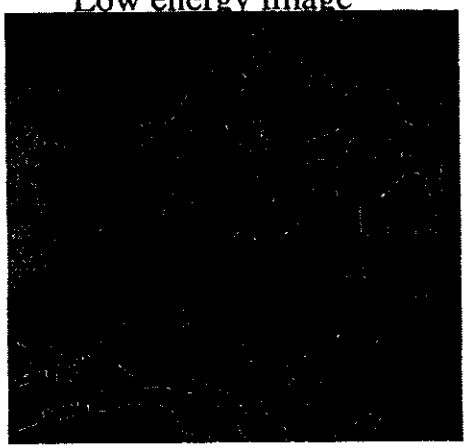

High energy image

Micro pattern detectors

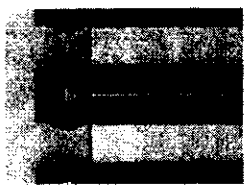

Micro strip chambers

A.Oed,
Nucl.Instrum.and Meth.
A 263 (1988)351

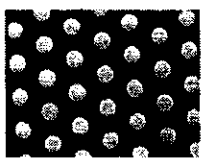

GEM

F.Sauli,NIM A386 (1997)531

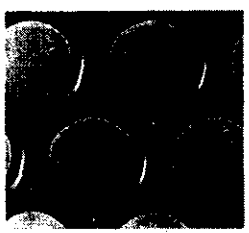

(Micro) CAT

F.Bartol et al,
J.Phys.III France 6 (1996)337

A.Sarvestani, R.H.Menk,
Nucl.Instrum.Methods
A 410 (1998)238

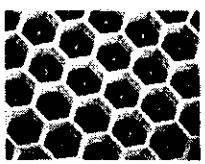

MIPA

P.Rehak et al,IEEE
Nucl.Sci.Symposium Seattle 1999

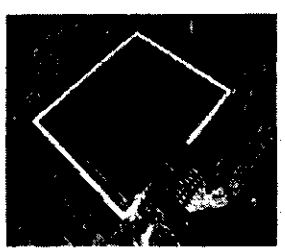

MicroMegas

Y.Giomataris et al,.
Nucl.Instrum.Methods
A376 (1996)29

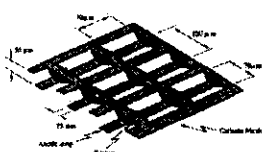

Micro wire chamber

B.Adeva et al,NIM.A435(199)402

Max rate ca 10 Mhz due to charge spread

Micro Pattern detectors

Micro CAT

Micro CAT used as
- shielding grid in ionization mode
  (required for fast signals)
- high rate gas gain amplification device

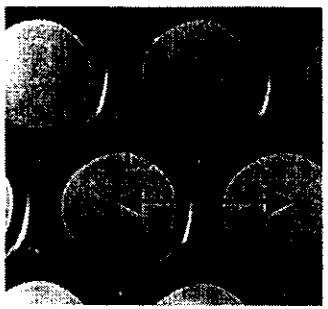

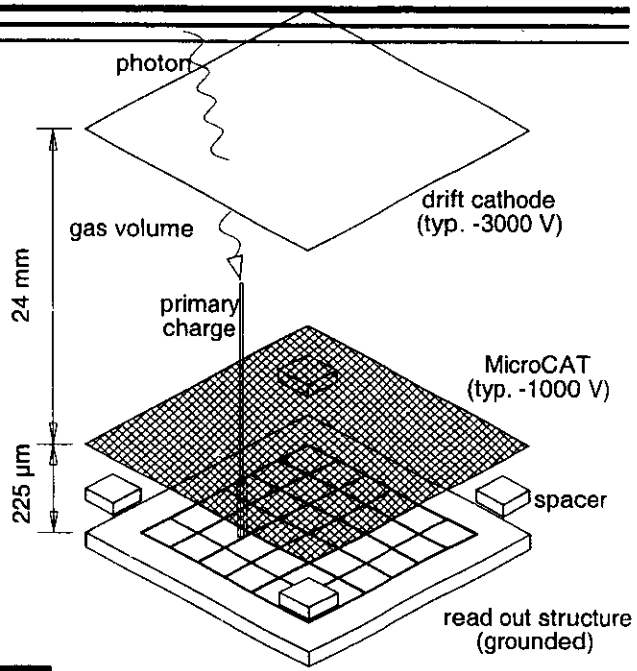

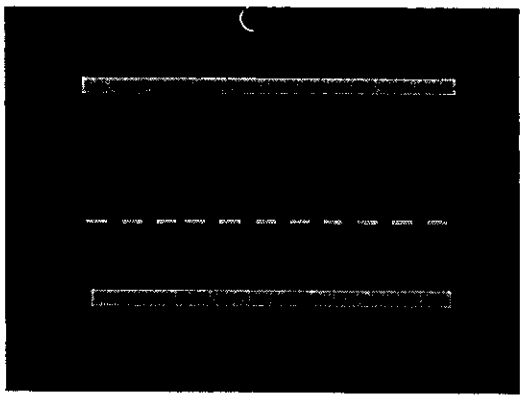

2-d pixel detector

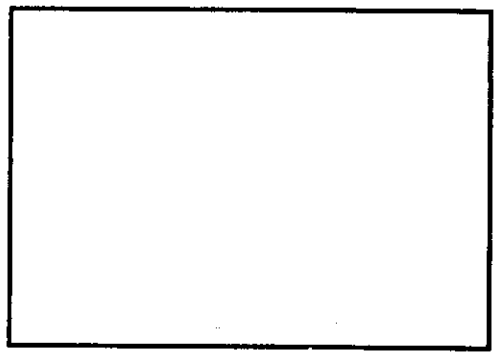

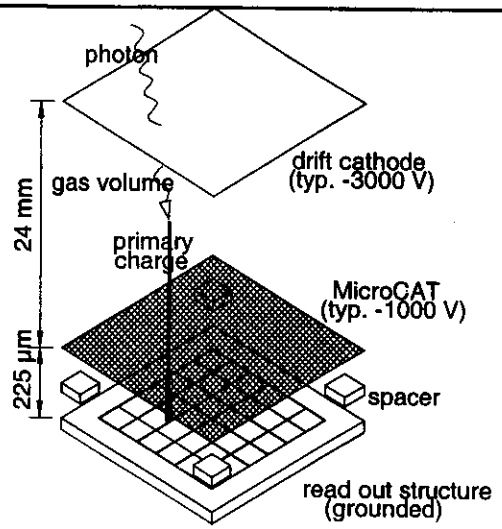

Features:

- single photon counting pixel detector
- interpolating read out by charge division
- DQE(f=0) ca 80 % for 8-16 keV (< 1Mhz)
- Spatial resolution ca 200 µm
- 5.6*5.6 cm^2
- 64 channels preamp-shaper-fadc
- energy resolution 25 % local
- spot rate 0.5 - 1 Mhz
- fast framing some µs

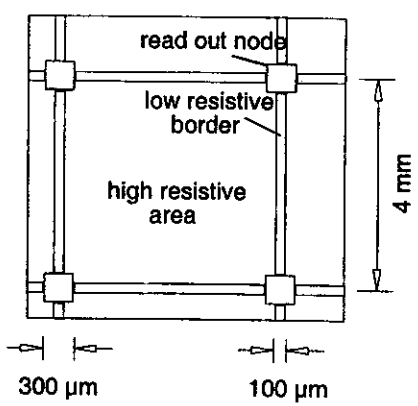

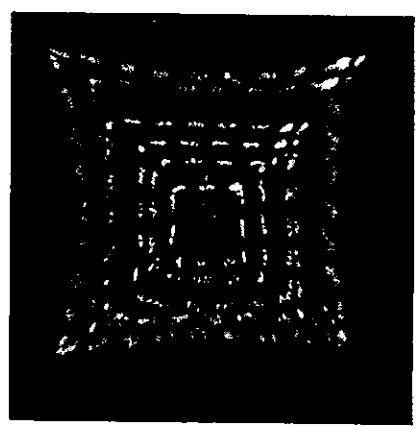

Image distortion is due to simple reconstruction

Ref:"Biological X-ray diffraction measurements with a novel two-dimensional gaseous pixel detector", A. Sarvestani, H. Amenitsch, S. Bernstorff, H.-J. Besch, **R. H. Menk**, A. Orthen, N. Pavel, M. Rappolt, N. Sauer and A.H. Walenta, J. Synchrotron Rad. (1999). 6, 985-994

2-d pixel detector

DSPC lipid (1,2-Distearoyl
-sn-Glycero-3-Phosphatidylcholin)

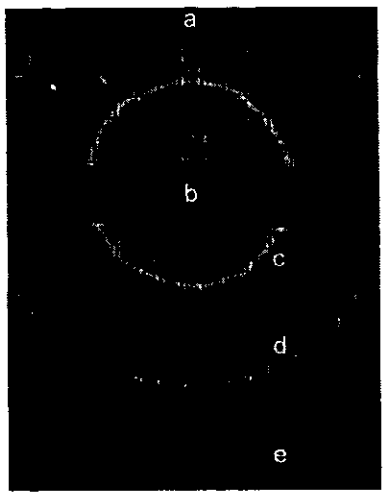

Data crunching

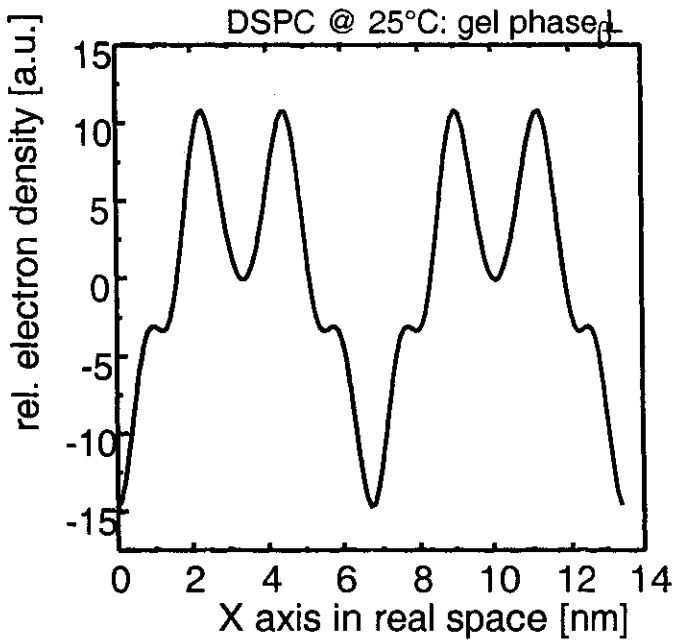

Time resolved measurements (repetitive)

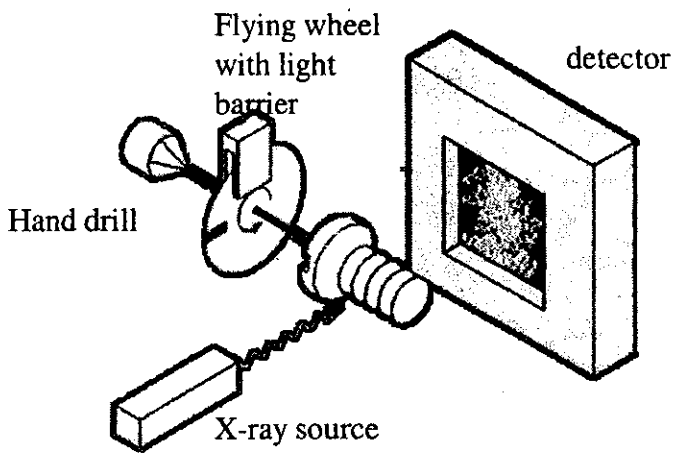

Time framing
18 µs

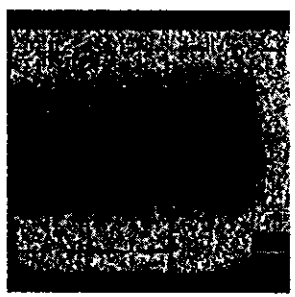

Each frame
is a set of
projections

Real time tomography

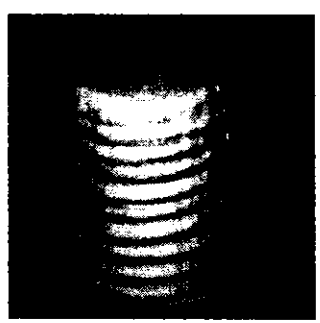

SAXS detector EU project CT 961694

- Initiated 1997
- Approved April, 1998 and funded since July, 1998
- Partners
  - Daresbury , Coordinator,Lewis
  - Sincrotrone Trieste, technical coordination,Menk
  - Hasylab, Gehrke
  - ESRF,Riekel
  - University Siegen,Germany, Walenta
  - IBR,Austria, Laggner

Features:

- multi channel ionization chamber
- DQE(f=0) ca 80 % for 8-16 keV (>10 photons/us)
- Spatial resolution ca 150 μm
- 400 e- noise equivalent (VLSI)
- allows gas gain operation in combination with integration
  - single photon resolution
  - max count rate 10^{12} photons mm^{-2} s^{-1}

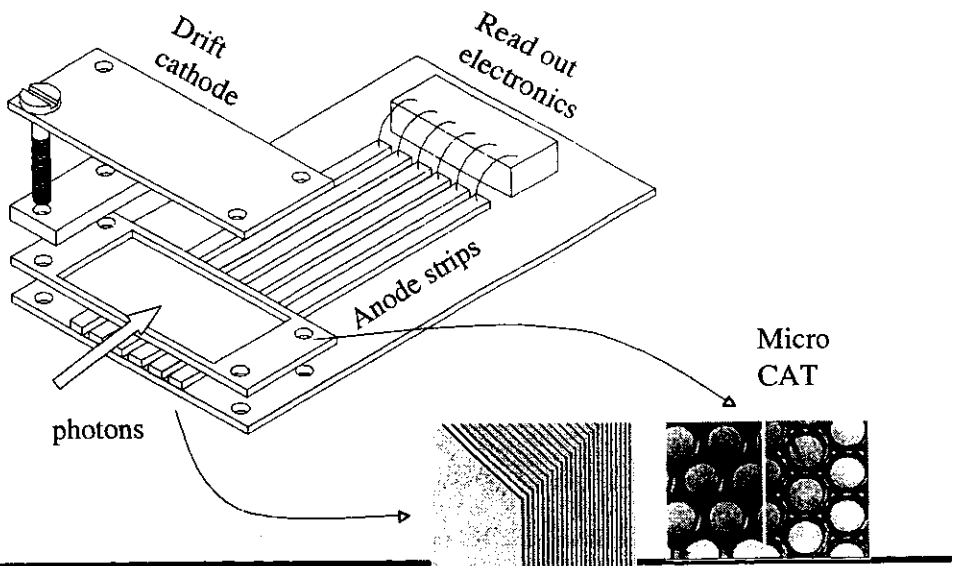

Ref: "Gas gain operations with single photon resolution using an integrating ionization chamber in SAXS experiments" R.H.Menk, A.Sarvestani, H.J.Besch, A.H.Walenta, H.Amentisch, S.Bernstorff, NIM A 440 (2000), 181-191

SAXS detector EU project CT 961694

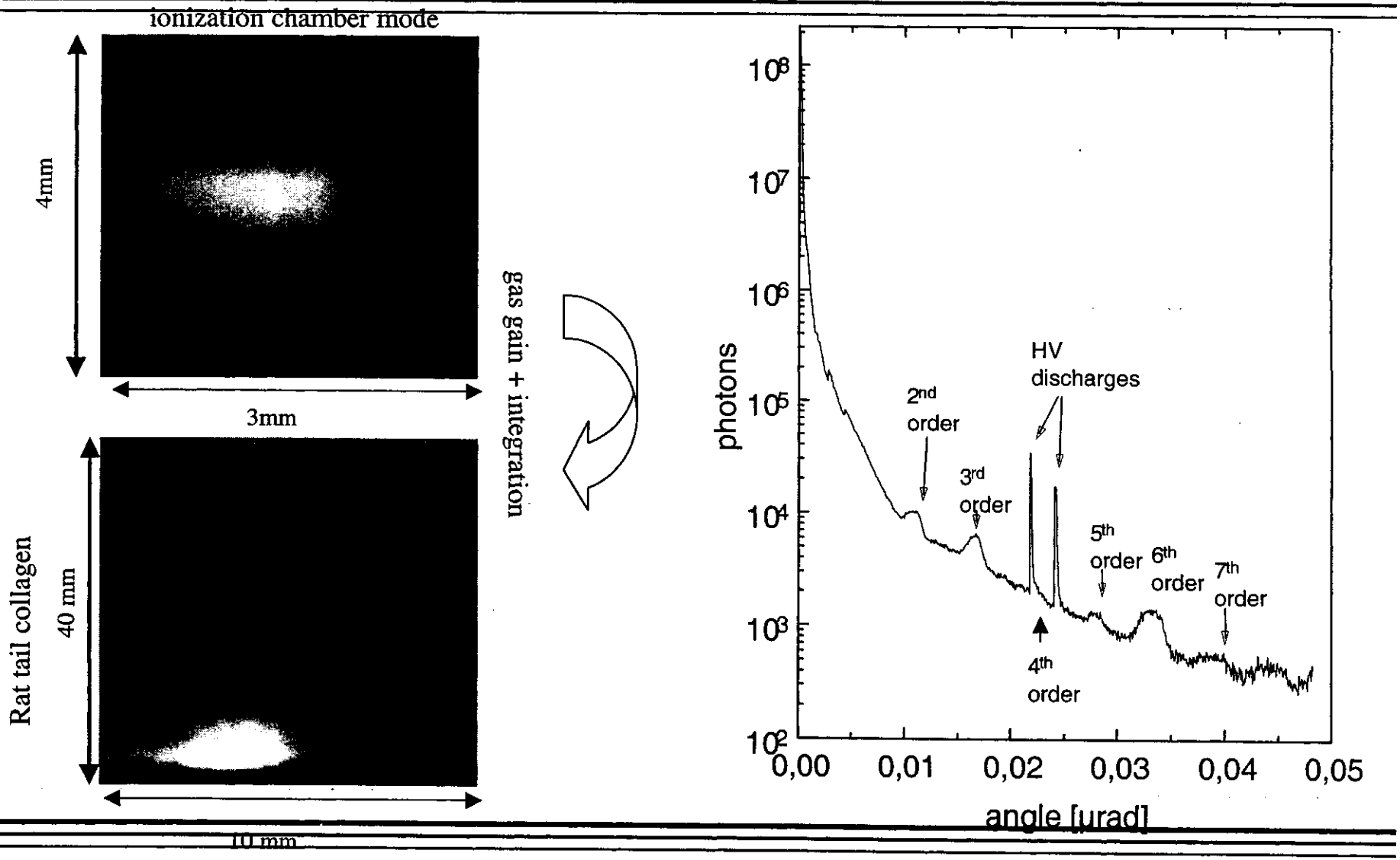

Which devices are available?

Integrating detectors

- CCDs
- TFTs
- Germanium .....
- Phosphors (image plate)

Solid state

counting detectors

- Si Strip detector
- photo multipliers
- Micro channel plates....

Spectroscopic detectors

- Si Drift chambers
- Germanium detectors
- Silicon diodes
- ....

Si drift chamber (Strueder et al , Max Planck institute Munich)

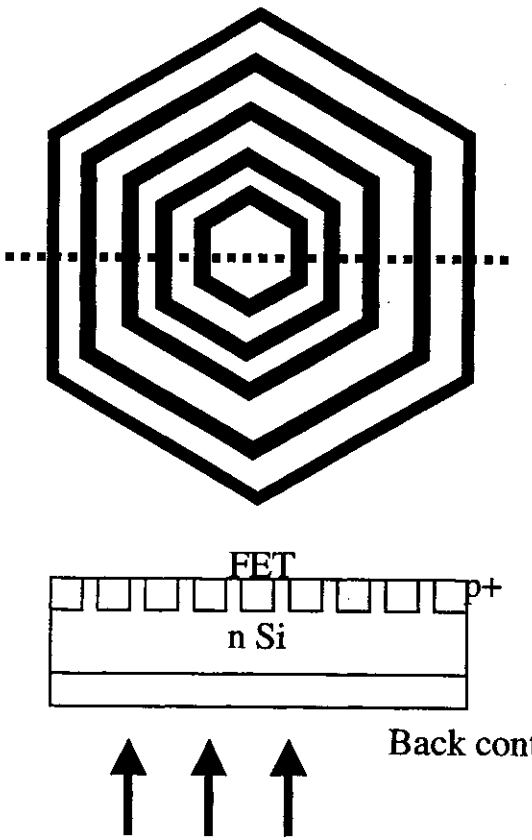

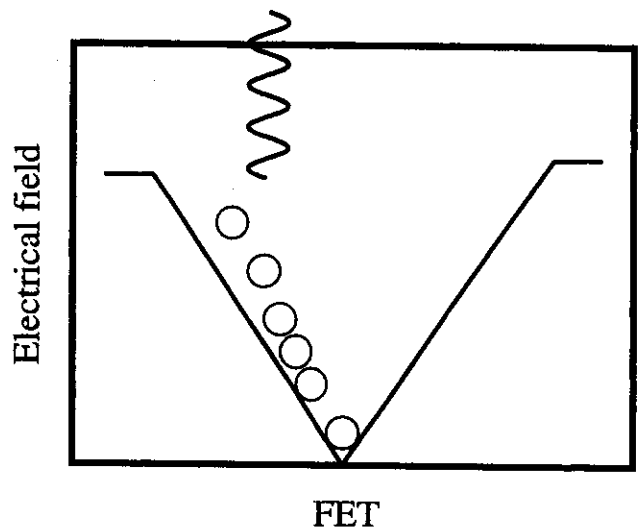

- Active area 5 mm^2
- Energy resolution 145 eV @ 5.9 keV
- ENC = 9 rms!

Low capacity -> low noise and fast device

Syrmep collaboration Si-strip detector

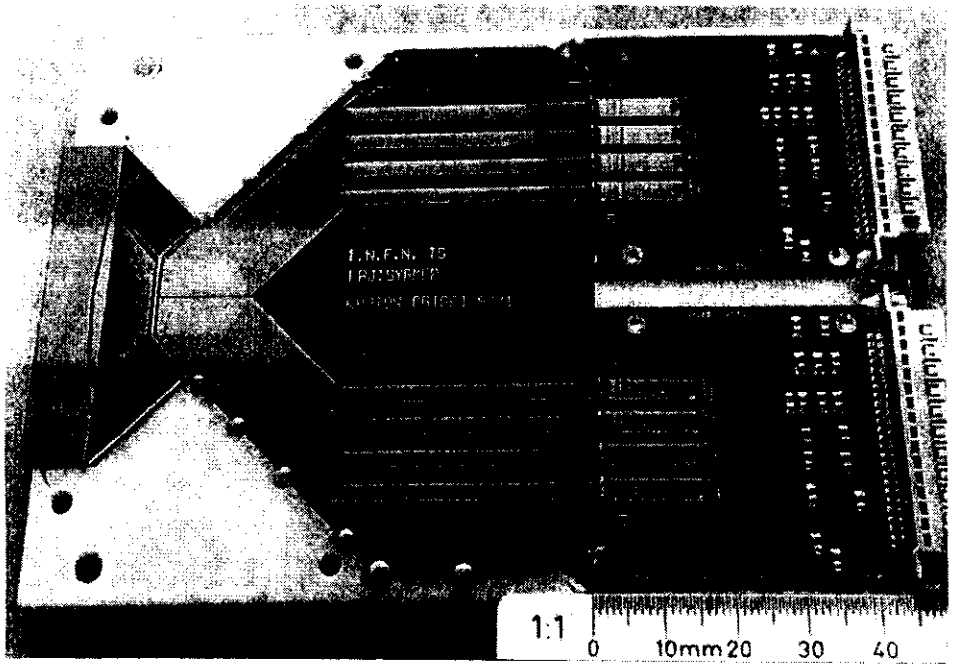

Bulk contact on the junction side
via a forward biased p^+ implant

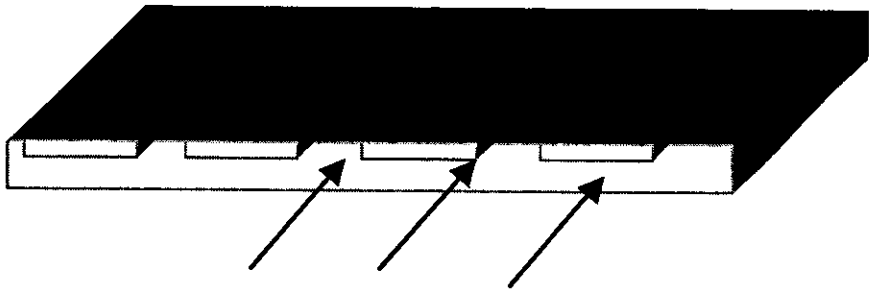

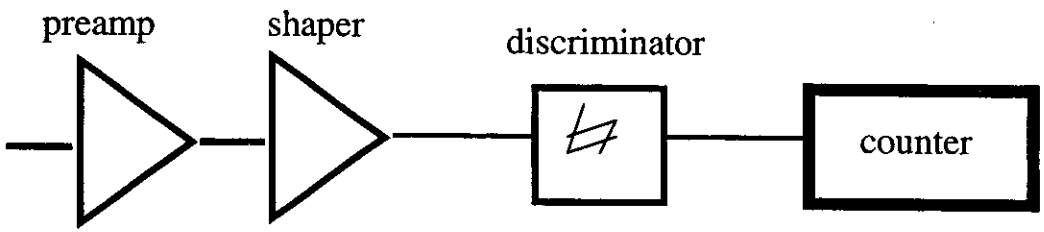

Real breast tissue recorded with the Syrmep detector

Full-field digital detector CCDs, flat panels

- Flat panel TFT amorphous silicon (indirect conversion)
- Charge-coupled device (indirect conversion)
- Flat panel TFT amorphous selenium (direct conversion)
- (Photostimulable phosphor - Imaging plate)

Direct conversion Indirect conversion

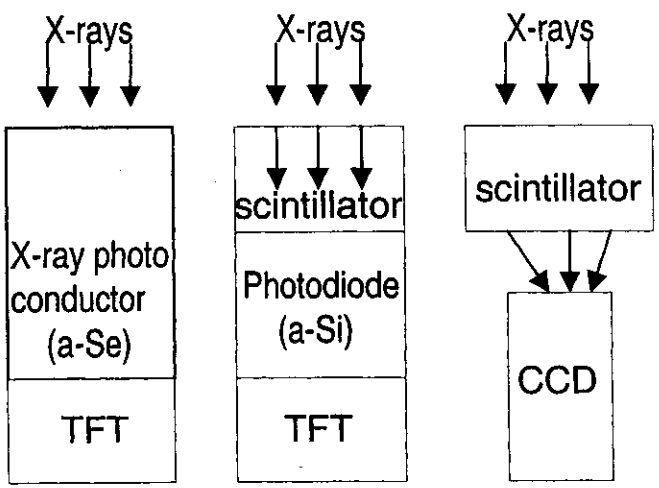

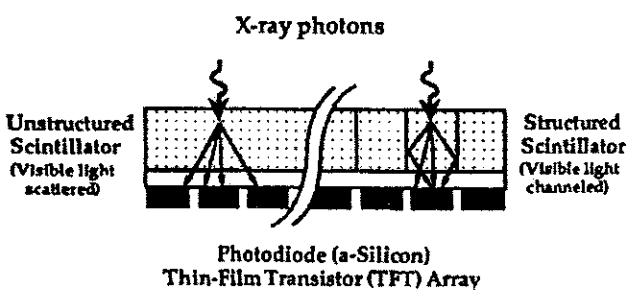

Ref: Feig SA and Yaffe MJ Digital Mammography. Radiographics. 18: 893-902 1998.
Yaffe MJ, Rowlands JA. X-ray detectors for digital radiography. Phys Med Biol 42 1-39, 1997

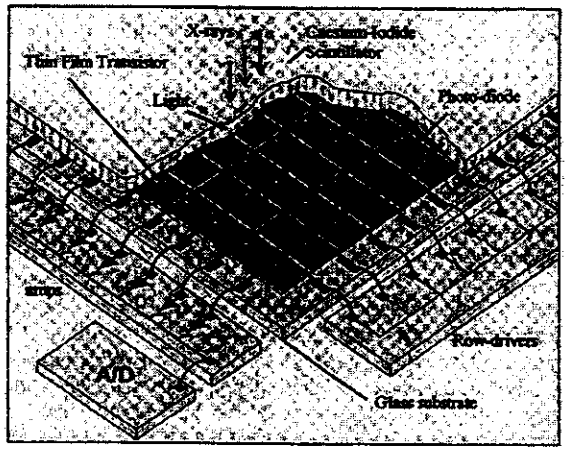

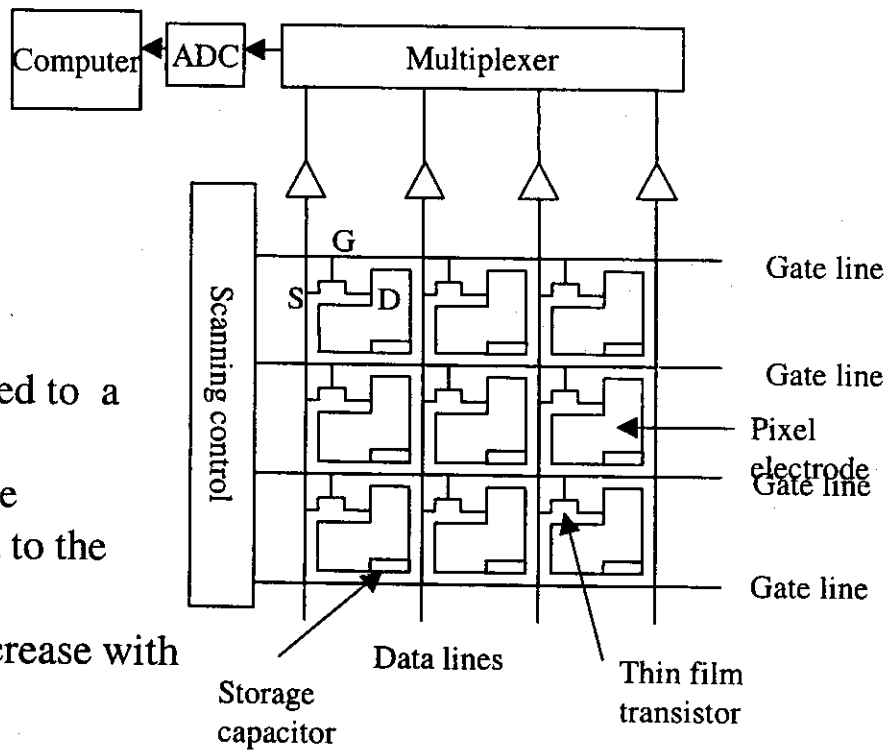

Amorphous silicon array (a-Si:H):

- Indirect conversion
- Each pixel consists of (a-Si) photodiode coupled to a TFT (a-Si Field-Effect Transistor) .
- The FET acts as a switch (controlled by the gate potential); it connects the photodiode (connected to the drain) to the source
- Active fraction (fill factor) less than 100% (decrease with decreasing pixel size)
- Lag in the image signal

Correction of CCd images

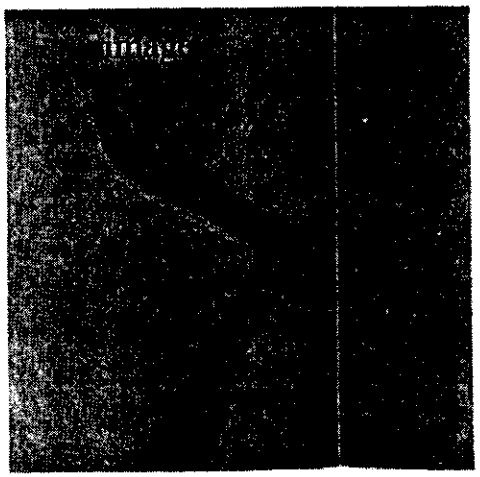

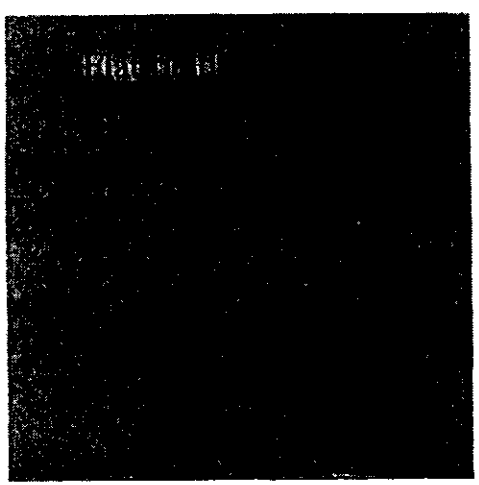

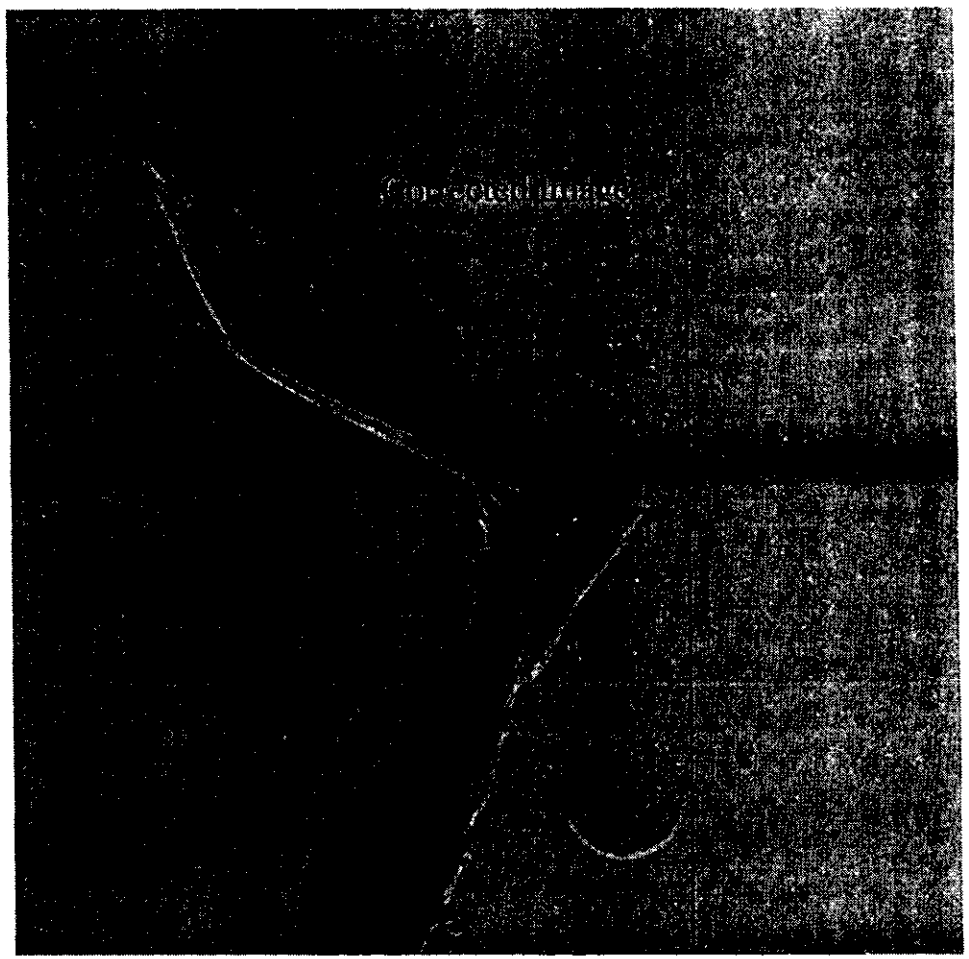

Detector : photonics science
beam line: Syrmep

Multi-channel electron analyzers

ESCATON 96
Superesca BL

ESCATON 16
Spectromicroscophy

2-d analyzer

Multi-channel parallel read-out enables

- High speed Photoelectron spectroscopy
- Acquisition without dead time
- Acquisition of one energy spectrum at a time without energy scan

Fondo Trieste

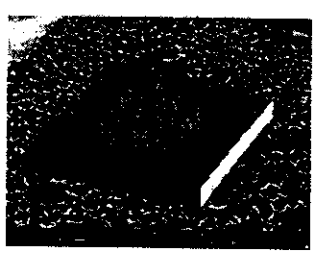

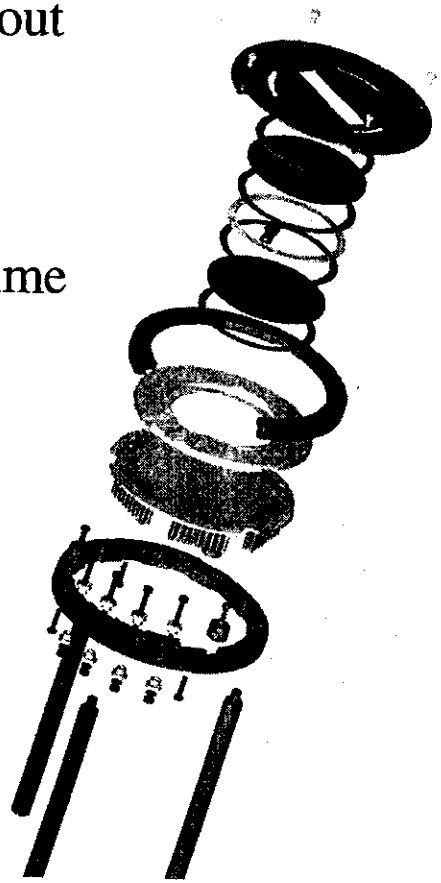

Ref:"An embedded control and acquisition system for multichannel detectors", L.Gori, **R.Tomassini, G.Cautero**, D.Giuressi, M.Barnaba, A.Accarodo, S.Caratto, G.Paolucci, NIM A431 (1999), 338-346

ESCATON 96

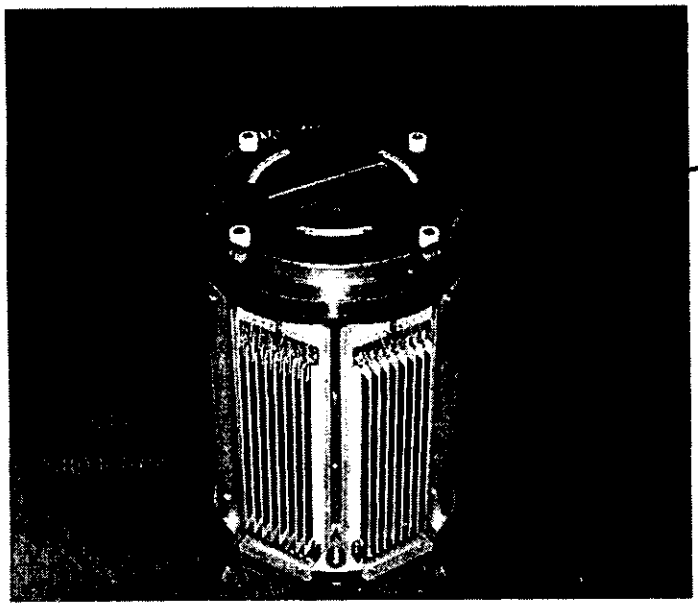

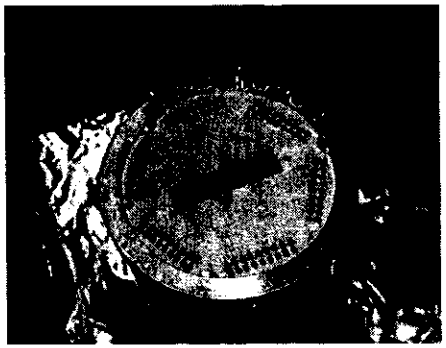

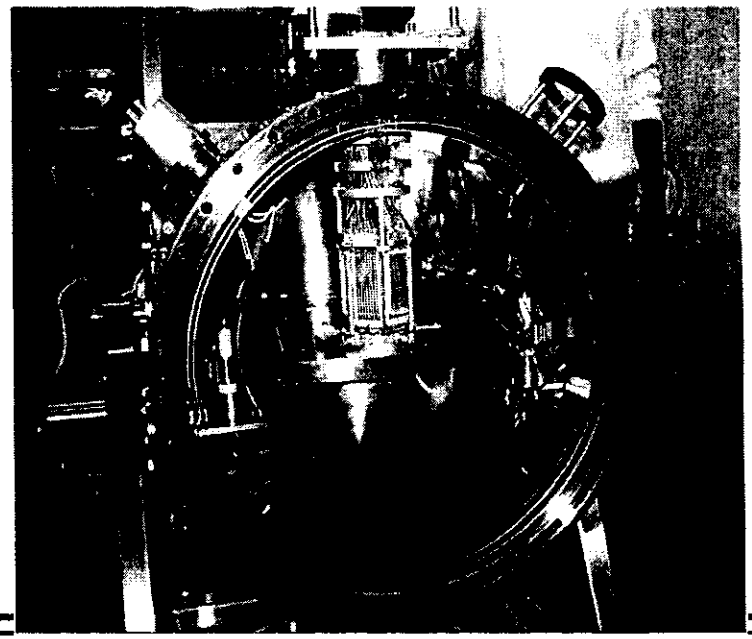

Ralf-Hendrik Menk Detectors

Front end electronics

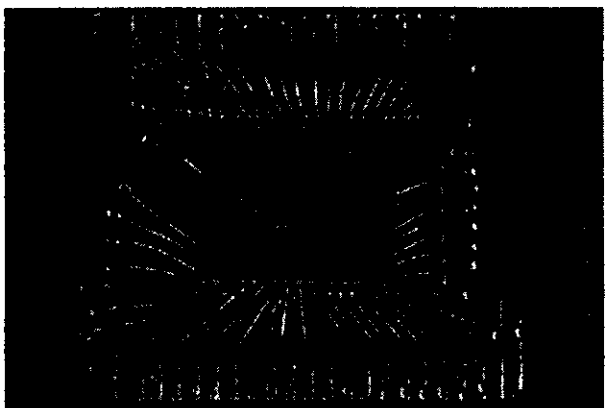

CMOS VLSI "MICA"
- 16 channel charge amplifier array
- Sensitivity 10^4 e^-
- 50 ns double pulse resolution
- Programmable threshold

- Eurocard form 4 layers PCB
- 16 coaxial 50Ω inputs
- Mixed CMOS/ECL design
- Multiple onboard supply regulators
- Double Π cell RLC supply filters
- High speed balanced PECL outputs

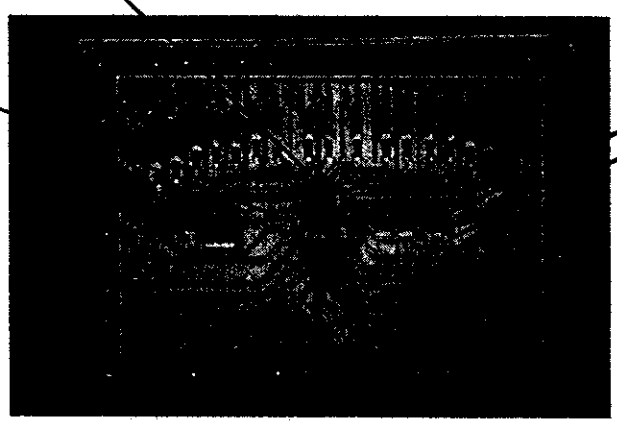

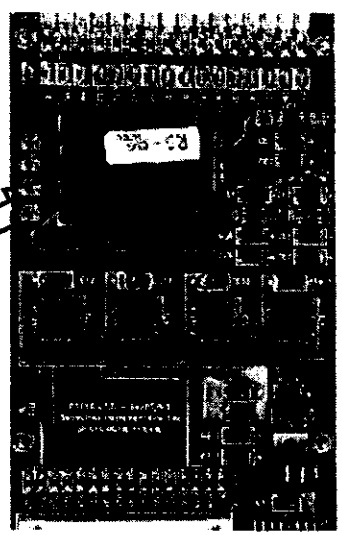

Thick Film Hybrid Module "CHYBA"
- 54 pin metal package
- High reliability input protection
- Sensitivity 10^6 e^-

But....

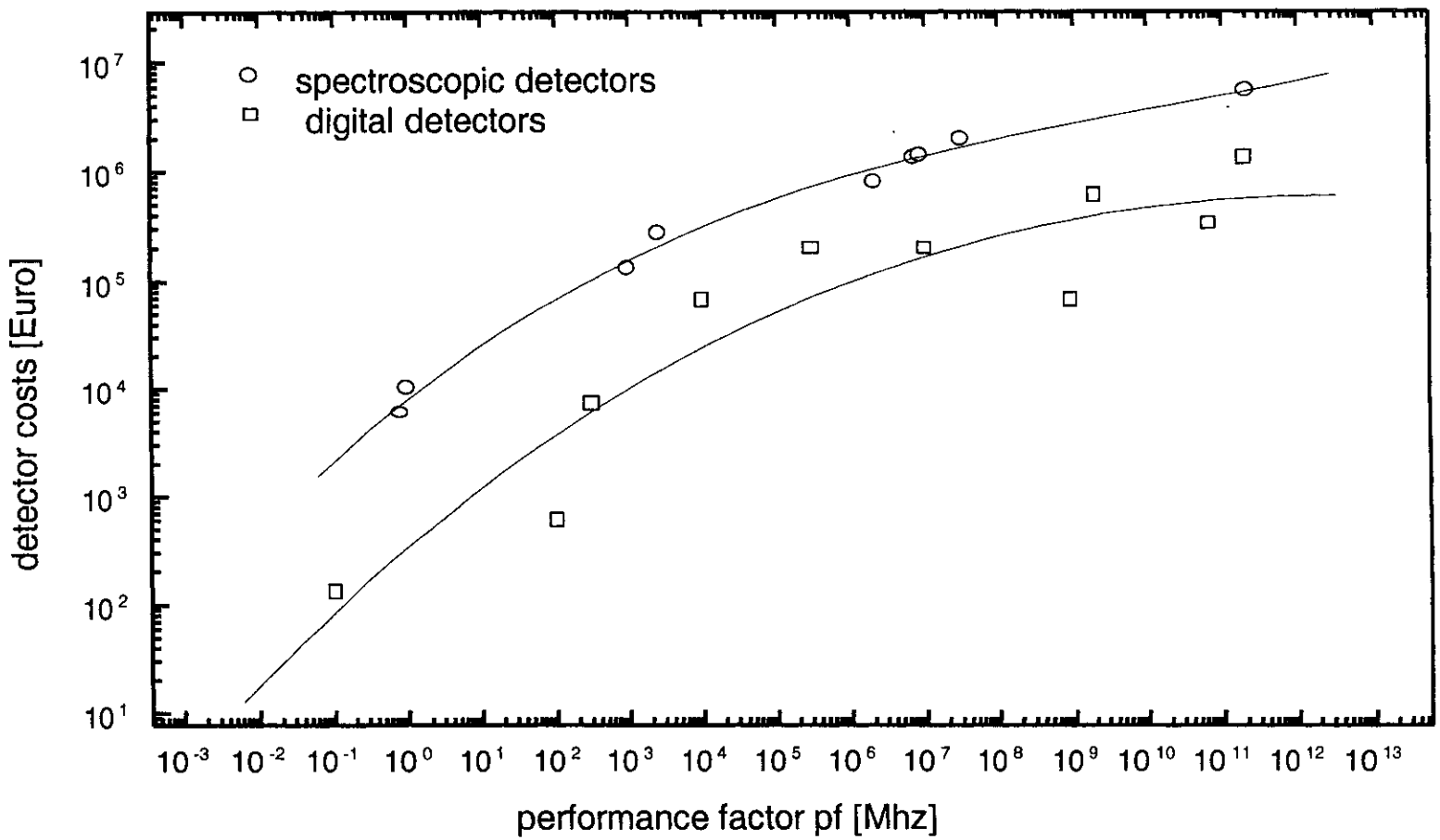
spectroscopic detectors
digital detectors
detector costs [Euro]
performance factor pf [Mhz]
10^7
10^6
10^5
10^4
10^3
10^2
10^1
10^-3 10^-2 10^-1 10^0 10^1 10^2 10^3 10^4 10^5 10^6 10^7 10^8 10^9 10^10 10^11 10^12 10^13